



Department of Aerospace Engineering
and Applied Mechanics
University of Cincinnati

NASA-CR-168003
19830003775

THREE DIMENSIONAL FLOW COMPUTATIONS IN
A TURBINE SCROLL

BY

A. HAMED AND C. ABOU GHANTOUS

LIBRARY COPY

AUG 4 1987

LANGLEY RESEARCH CENTER
LIBRARY, NASA
HAMPTON, VIRGINIA

Supported by:

NATIONAL AERONAUTICS AND SPACE ADMINISTRATION

Lewis Research Center

Grant No. NAG3-52



3 1176 01318 5260

NASA CR 168003

THREE DIMENSIONAL FLOW COMPUTATIONS IN
A TURBINE SCROLL

by

A. Hamed and C. Abou Ghantous

Department of Aerospace Engineering and Applied Mechanics
University of Cincinnati
Cincinnati, Ohio 45221

Supported by:

NATIONAL AERONAUTICS AND SPACE ADMINISTRATION

Lewis Research Center

Grant No. NAG3-52

N83-12045[#]

1 Report No CR 168003		2 Government Accession No		3 Recipient's Catalog No	
4 Title and Subtitle THREE DIMENSIONAL FLOW COMPUTATIONS IN A TURBINE SCROLL				5 Report Date August 1982	
				6 Performing Organization Code	
7 Author(s) A. Hamed and C. Abou Ghantous				8 Performing Organization Report No	
9 Performing Organization Name and Address DEPT. OF AEROSPACE ENGINEERING & APPLIED MECHANICS UNIVERSITY OF CINCINNATI CINCINNATI, OHIO 45221				10 Work Unit No	
				11 Contract or Grant No NAG3-52	
12 Sponsoring Agency Name and Address NATIONAL AERONAUTICS AND SPACE ADMINISTRATION LEWIS RESEARCH CENTER CLEVELAND, OHIO 44135				13 Type of Report and Period Covered	
				14 Sponsoring Agency Code	
15 Supplementary Notes					
16 Abstract <p>The present analysis is developed to calculate the compressible three dimensional inviscid flow in the scroll and vaneless nozzle of radial inflow turbines. A Fortran computer program which was developed for the numerical solution of this complex flow field using the finite element method is presented.</p> <p>The program input consists of the mass flow rate and stagnation conditions at the scroll inlet and of the finite element discretization parameters and nodal coordinates. The output includes the pressure, Mach number and velocity magnitude and direction at all the nodal points.</p> <p>The report includes the computer program, the analysis, a description of the solution procedure, and a numerical example.</p>					
17 Key Words (Suggested by Author(s))				18 Distribution Statement Unclassified - unlimited. STAR CATEGORY 02	
19 Security Classif (of this report) UNCLASSIFIED		20 Security Classif (of this page) UNCLASSIFIED		21 No of Pages 52	22 Price*

* For sale by the National Technical Information Service Springfield Virginia 22161

TABLE OF CONTENTS

	<u>Page</u>
SUMMARY	1
INTRODUCTION	2
MATHEMATICAL ANALYSIS	2
INPUT	5
OUTPUT	7
PROGRAM DESCRIPTION	8
PROGRAM LISTING	12
NUMERICAL EXAMPLE	33
REFERENCES	35
TABLES AND FIGURES.	36
APPENDIX A - DEVIATION OF THE ELEMENT EQUATION	47
APPENDIX B - THE MATCHING CONDITIONS AT THE SPITTING SURFACE	50
APPENDIX C - NOMENCLATURE	52

LIST OF FIGURES

<u>Figure</u>		<u>Page</u>
1	Scroll Schematic Showing the Coordinates and the Splitting Surfaces	40
2	Structure of the Program	41
3	Nodal Placement on the Scroll Surface ABC . . .	42
4	Nodal Placement in Scroll Cross Section	43
5	Velocity Potential Contours on Scroll Surface AED	44
6	Contours of Computed Circumferential Velocity Component	45
7	Measured Circumferential Velocity Component (Ref. 5)	46

SUMMARY

The present analysis is developed to calculate the compressible three dimensional inviscid flow in the scroll and vaneless nozzle of radial inflow turbines. A Fortran computer program which was developed for the numerical solution of this complex flow field using the finite element method is presented.

The program input consists of the mass flow rate and stagnation conditions at the scroll inlet and of the finite element discretization parameters and nodal coordinates. The output includes the pressure, Mach number and velocity magnitude and direction at all the nodal points.

The report includes the computer program, the analysis, a description of the solution procedure, and a numerical example.

INTRODUCTION

Existing quasi-three-dimensional turbomachinery flow field solutions are applicable to radial inflow turbine rotors but not to its scroll. Most analytical studies of the flow in the scroll [1, 2] are based on the assumption of one dimensional flow and the conservation of mass and angular momentum. A two dimensional study of the flow field in the scroll and nozzles was reported in reference [3]. Another two dimensional study of the velocity components in the cross-sectional planes of the scroll was reported in reference [4]. These two analytical investigations provided insight into the influence of the scroll and nozzle vane geometries on the flow field but together do not constitute a quasi-three-dimensional solution. Experimental measurements of the velocity components in the radial turbine scroll [5] indicate that actually the three dimensional scroll flow fields are very complex.

This work presents a method for the analysis and a code for computing the compressible inviscid three dimensional flow field in the scroll and vaneless nozzle of a radial inflow turbine. The finite element method is used in the numerical solution in order to model the complex geometrical shape of the flow boundaries.

MATHEMATICAL ANALYSIS

The three basic steps involved in the finite element method are the domain discretization, obtaining the integral statement of the problem and the appropriate choice of the local approximation in each element [6, 7]. In this study, the three dimensional flow field is formulated in terms of the potential function and Galerkin's method is used to obtain the integral statement.

For steady flow, the equation of conservation of mass is expressed in terms of the potential function ϕ as follows:

$$\nabla \cdot (\rho \nabla \phi) = 0 \quad (1)$$

The unknown velocity potential solution is approximated in each element by

$$\phi^e = [N] \{\phi\}^e \quad (2)$$

where $\{\phi\}^e$ is the column vector of the potential function values ϕ_i , at the nodes of the element e , and $[N]$ is the row vector of the interpolation functions N_i .

Galerkin's method requires the residual of the substitution of equation (2) into equation (1) to be orthogonal to the interpolation functions

$$\int_V N_i \nabla \cdot (\rho \nabla \phi) dV = 0 \quad (3)$$

Applying Green's theorem to equation (3) leads to the following relation which involves the boundary conditions:

$$\int_V \nabla N_i \cdot (\rho \nabla \phi) dV = \int_A N_i \rho \nabla \phi \cdot dA \quad (4)$$

The integrals in the above equations are evaluated over the volume V and surface A of all the solution domain. The right-hand side of equation (4) represents the weighted average of the mass flow across the solution domain boundaries. The solid boundaries contribution to equation (3) is equal to zero because of the no-flux condition.

Equation (4) holds for the entire solution domain and also for an arbitrary finite element e . The substitution of equation (2) into equation (4) gives the following element equation:

$$\int_{V^e} \nabla N_i \cdot (\rho \nabla [N] \{\phi\}^e) dV = \int_{A^e} N_i \rho \frac{\partial \phi}{\partial n} dA \quad (5)$$

Equation (5) is nonlinear for compressible flow where the density is given by:

$$\rho = \rho_0 \left[1 + \frac{\gamma-1}{2\gamma} \frac{(\nabla\phi)^2}{RT_0} \right]^{-1/\gamma-1} \quad (6)$$

The numerical solution to equations (5) and (6) is obtained iteratively by allowing the density, ρ , in equation (5) to lag one iteration behind the potential flow field solution. The assembly of all the linearized element equations in the flow field results in a set of linear algebraic equations which can be expressed as follows:

$$[K] \{\phi\} = \{P\} \quad (7)$$

The Gauss elimination method is used in the solution of the linearized equations.

The matrix of coefficients is updated at each iteration but the load vector remains unchanged, as it is determined by the mass flow rate in the scroll. Appendix A gives a detailed derivation of the element equations and of the coefficients of the stiffness matrix.

The Splitting Surfaces

The choice of the potential function as a dependent variable is generally suitable for three dimensional flow field solutions in simply connected domains. However the domain in the scroll problem is multi-connected leading to a mathematically non-unique solution for the potential function. In the present analysis, two coincident surfaces are introduced in the solution domain to make it simply connected. The splitting surfaces extend from the scroll lip, which is the end of the metal between the inlet section and the last scroll section, to the vaneless nozzle exit station as shown in Fig. 1. In the flow field discretization, two sets of nodes are placed on the opposite sides of the splitting surfaces and a discontinuity in the velocity potential field is allowed across. Additional matching conditions are therefore required to insure the continuity in the velocity field across these boundaries as described in Appendix B.

INPUT

The input data to the program is read in subroutine INPUT. It consists of the geometrical data and the performance parameters for a given scroll. Any consistent set of units can be used for the input variables. Other input parameters are related to the numerical solution procedures and to produce the desired output. Following is a description of the input data in alphabetical order.

BANDWD	An integer equal to the band width of the matrix of coefficients.
GAMA	Specific heat ratio.
EPSILN	A small number describing the tolerance which is used to determine the convergence of the numerical solution based on the normalized density change.
INDATA	Integer to indicate if it is desired to print out the input data. INDATA = 0 will not produce a printout of the input data while INDATA = 1 will produce a printout of the input data.
ITERMX	The number of iterations not to be exceeded in the solution. Incompressible flow solution is obtained if ITERMX = 1.
J1(I)	An array of the global number of the first node of every cross section I
LBC(I),MBC(I), NBC(I)	Arrays of the nodal points of the surface element I.
MSRATE	The mass flow rate in the scroll (kg/sec or slg/sec).
MS1	The number of surface elements at the inlet station.
MS2	Total number of surface elements at inlet section and the first splitting surface.
MS3	Total number of surface elements at inlet section and the two splitting boundaries.

MSTOT	Total number of surface elements at inlet, exit and splitting boundaries.
MTOT	Total number of volume elements.
MV(I)	The global number of the volume element which contains the splitting surface element I (I = MS1+1 to MS3).
NANZ	The number of nodal points in the axial direction in the nozzle.
NC	Total number of cross sections in the scroll and inlet passage.
NRNZ	The number of nodal points in the radial direction in the nozzle.
NODE(I,J)	Array of the global number of the nodes, I = 1,2,3,4, of the element J. J = 1, MTOT.
NTOT	Total number of nodes.
NU(I)	An array of the number of nodes at every cross section I.
R	Gas constant: (J, °K or lb ft/slg °R).
STAGP	Stagnation pressure (newton/m ² or lb/ft ³).
STAGT	Stagnation temperature (°K or °R).
THETA(I)	An array of the angles between every cross section plane and the x-z plane measured from the positive x-direction.
X(I),Y(I), Z(I)	Arrays of the Cartesian coordinates of all the nodal points.

The reading formats of the input variables are illustrated in Table 1.

Input Preparation

The solution region includes the inlet, the scroll and the vaneless nozzle. The splitting boundaries should extend from the lip (the last metal part between the inlet and the last scroll section) to the exit station of the vaneless nozzles.

It can have any shape that is consistent with the discretization pattern. The discretization pattern and system topology is arbitrary. The surface elements at the inlet, exit and the splitting boundaries are inputted in one array. They are numbered sequentially up to MS1 on the inlet section, then up to MS2, then MS3 on the two splitting boundary surfaces, then up to MSTOT on the exit station. The volume elements associated with these surface elements are inputted in the array MV(I), I = 1, MSTOT. The angular coordinates THET(I), of the cross sectional planes, including those at inlet, are only used to evaluate the through flow velocity V_T and the radial velocity V_r from the computed velocity components in Cartesian coordinates after the convergence of the numerical solution.

It is up to the user to select the number of cross sections and the nodal points per cross section. The band width is equal to the maximum difference between the global number of any two nodes of the same element. The system topology can be specified in such a manner as to minimize the band width of the matrix of coefficients in the numerical solution. For the purpose of organizing the printout of the output, the nodes in each section N(J) are numbered sequentially starting with JI(J), J = 1, NC.

OUTPUT

A sample output is given in Table 2 for the scroll of the numerical example. The first set of output consists of a printout of the input parameters. The second set of output consists of a listing of the potential function, the through flow velocity, the cross velocities, the total velocity, the Mach number, the pressure and density normalized by their inlet stagnation values. The computed flow data are listed for every section starting at inlet so that they can be easily interpreted.

Error Messages

The following error conditions lead to program termination.

1. ELEMENT NUMBER XXX HAS A ZERO VOLUME
(LESS OR EQUAL TO XXX)
CALCULATION IS STOPPED.

The message is printed in subroutine MATVEC during the first iteration as the element volumes are evaluated in ascending element order. Check the coordinates of NODE (I, ELEMENT NUMBER XXX) for error.

2. WARNING:
SINGULARITY IN ROW XXX
CALCULATION IS STOPPED.

This message is printed in subroutine GAUSS if the diagonal element of the matrix of coefficient is less than 10^{-5} . The row number is printed to be used for the identification of the corresponding nodal point. Check the topology of the elements associated with this node in the discretization pattern.

PROGRAM DESCRIPTION

The main program is designed to obtain the potential flow solution in a radial inflow turbine scroll using the finite element technique. The program is built from four major subroutines: MATVEC, SPLIT, GAUSS and PHYSIC, two edit subroutines: INPUT and OUTPUT, and four supplementary subroutines: VOLELM, NUMBER, AR and COFACT which are called inside the major subroutines at various steps for side calculations. The structure of the program is shown on Fig. 2.

Descriptions of the Subroutines

I. Major subroutines:

MATVEC: The stiffness matrix elements, K_{ij} , and the load vector, P_j , are calculated in this subroutine. In addition, the volume of the elements are calculated and stored in the array VOL(I) so that it can be used in other subroutines and

in subsequent iterations. The coefficients of the element stiffness matrix, K_{ij} are calculated using Eq. (A.8). Subroutine COFACT is called to calculate the coefficients a_k , b_k and c_k (Eq. A.7). The load vector components P_j are calculated using Eqs. (A.10).

SPLIT: The matching conditions across the splitting surfaces, as explained in Appendix B are implemented in this subroutine.

GAUSS: The solution for the potential function at the nodal points (I) is obtained in this subroutine using the Gauss elimination method. The matrix of coefficient is bounded, but nonsymmetric due to the application of the matching condition at the splitting boundary. Since the solution to the potential function is unique within an arbitrary constant, the magnitude of the potential function at the first node is arbitrarily fixed at -1.

PHYSIC: The physical properties of the fluid are calculated in this subroutine which is called after the nodal potentials are determined. The properties calculated at each node are: the velocity components as defined by Eq. (A.), the Mach number and the normalized pressure and density. The difference between the element density of two subsequent iterations are also evaluated in this subroutine to be used in the convergence criteria.

II. Edit subroutines:

INPUT: Called first in SOLVE to read and write the input data. It also initializes the normalized density in each element to unity.

OUTPUT: After the convergence of the solution, the velocity potential and flow properties are printed at all the nodes. The printout is organized so that the data of each cross section is identified and printed separately.

III. Side calculations subroutines:

NUMBER is called by SPLIT to rearrange, at the element level, the nodes of the elements with surfaces on splitting boundary, such that the first three nodes of an element are on the splitting boundary. The nodes global numbers are then stored in the array NSB(I,J), where I is the number of the surface element on the splitting boundary and J = 1,2,3,4 are the global numbers of the three nodes on the splitting boundaries followed by the fourth internal node.

VOLELM is a subroutine with double indices N and K. The first index N refers to the element, and the second is a flag. If the index N is equal to 2, the coefficients of the interpolation functions are calculated according to equation (A.7). If it is equal to 1, a similar procedure is followed for the volume elements which have three nodes on the splitting surface whose nodes are locally renumbered and identified by the number of the surface element. If the second index is equal to zero, the volume of the element is also calculated according to equation (A.9). The volume calculations are only performed during the first iteration, then stored in VOL(I) for subsequent use in later iterations.

IV. Dictionary of common block variables:

A(I,J)	Global matrix of coefficients for the potential function at the nodes.
ART(I)	Area of surface element I (at inlet, exit and/or splitting boundary).
B(I,J)	The matrix B^e of the element nodal coordinates.
E(I)	The contribution of mass flow rate through a splitting boundary surface element, to the opposite surface element equation, in the global matrix of coefficients.
JI(J)	The global number for the first node in a scroll cross section J.

LBC(I),MBC(I), NBC(I), The nodal number for the three nodes of a surface element.

LOAD(I) An array containing the load vector.

MV(I) The global number of a volume element which contains the splitting boundary surface element I.

NU(J) Total number of nodes in the scroll cross section J.

NODE(I,K) The global number for the node of the volume element K, for the tetrahedral volume element I = 1,2,3,4.

NTL(I) An array containing the nodes on a splitting boundary arranged in descending order.

NSB(I,J) The global number of the nodes I of the element J with 3 nodes on the splitting surface.

PRTIAL(I,J) Partial derivatives of the interpolation functions N_J (J = 1,2,3,4) in Cartesian coordinates, $\frac{\partial}{\partial x}$ for I = 1, $\frac{\partial}{\partial y}$ for I = 2, $\frac{\partial}{\partial z}$ for I = 3).

VOL(I) Volume of an element I.

X(I), Y(I), Z(I) Coordinates of a node I.

PROGRAM LISTING

C
C
C

```

INTEGER BANDWD
REAL MSRATE,MSFLUX,LOAD,MACH2
COMMON/ASEMBL/H(4,4),VOL(3720),NODE(4,3720),A(960,406),NTL(155),
.   PRTIAL(3,4),ART(155),LBC(155),MBC(155),NBC(155),
.   X(960),Y(960),Z(960),LOAD(960),BANDWD,E(155),MV(155)
..  NSB(4,155),MS1,MS2,MS3,MSTOT,NTOT,JUMP1,JUMP2,NANZ,
.   NRNZ,POTEN(960)
COMMON/PHYSI/GAMA,R,STAGT,ERROR,VELO(3)
COMMON/INOUT/INDATA,MTOT,MSRATE,EPSILN,ITER,ITERMX,NC,STAGRO,
.   J1(60),NU(60),THETA(60),ROELEM(3720),NN

```

C
C
C
C

```

-->> WARNING; THE DIMENSION OF A(I,J) AS IN COMMON SHOULD AT LEAST
BE J=(BANDWD-1)*2.

```

C

```

CALL UNDFLW

```

C

```

CALL INPUT
ITER = 0

```

C

```

NN = BANDWD*2 - 1
DO 80 I=1,NTOT
801 LOAD(I) = 0.0

```

C

```

10 ITER = ITER + 1
DO 90 I=1,NTOT
DO 90 J=1,NN
90 A(I,J) = 0.0

```

C

```

BUILD UP THE STIFNESS MATRIX AND THE LOAD VECTOR.

```

C

```

CALL MATVEC

```

C

```

INTRODUCE THE SPLITTING SUFACE MATCHING CONDITIONS.

```

C

```

CALL SPLIT

```

C

```

SET THE FIRST DIAGONAL TERM IN STIFNESS MATRIX AND ITS
CORRESPONDING VALUE IN LOAD VECTOR EQUAL TO UNITY.

```

C

```

K = BANDWD + 1
F = ABS(A(1,BANDWD))
DO 160 I=K,NN

```

C

```
160 A(1,I) = 1.0E-15*A(1,I)/F
    A(1,BANDWD) = A(1,BANDWD)/F
    LOAD(1) = LOAD(1)/ABS(LOAD(1))
C
C   IMPOSE ZERO TANGENTIAL VELOCITY AT INLET SECTION.
C
    NODIN = NU(1)
    DO 170 I =2,NODIN
      L = K - I
      A(I,L) = A(I,L) + 1.0E+15
170 A(I,BANDWD) = A(I,BANDWD) - 1.0E+15
C
C   SEAK A SOLUTION FOR VELOCITY POTENTIALS; THE INLET SECTION IS
C   AN EQUIPOTENTIAL OF MAGNITUDE UNITY.
C
    CALL GAUSS
C
C   CALCULATE THE PHYSICAL PROPERTIES OF THE FLUID.
C
    CALL PHYSIC
C
C   TEST THE CONVERGENCE AND ITERATE.
C
    IF (ERROR.GT.EPSILN .AND. ITER.LT.ITERMX) GO TO 10
C
C   PRINTOUT THE CALCULATED PHYSICAL PROPERTIES IN THE CURRENT
C   ITERATION AT ALL NODES: VELOCITY POTENTIALS, VELOCITY COMPONENTS,
C   MACH NUMBER NORMALIZED PRESSURE AND DENSITY.
C
    CALL OUTPUT
C
    STOP
    END
```

SUBROUTINE MATVEC

THIS SUBROUTINE BUILDS UP THE STIFFNESS MATRIX AND THE LOAD VECTOR

INTEGER BANDWD

REAL MSRATE,MSFLUX,LOAD,MACH2

COMMON/ASEMBL/B(4,4),VOL(3720),NDDC(4,3720),A(960,406),NTL(155),

. PRTIAL(3,4),ART(155),LBC(155),MBC(155),NBC(155),
 . X(960),Y(960),Z(960),LOAD(960),BANDWD,E(155),MV(155)
 . NSB(4,155),MS1,MS2,MS3,MSTOT,NTOT,JUMP1,JUMP2,NANZ,
 . NRNZ,POTEN(960)
 COMMON/INOUT/INDATA,MTOT,MSRATE,EPSILN,ITER,ITERMX,NC,STAGRO,
 . J1(60),NU(60),THETA(60),ROELEM(3720),NN

1 FORMAT (1H1,20(/),25X,'ELEMENT NUMBER',I15,/,25X,
 . 'HAS A ZERO VOLUME (LESS OR EQUAL TO',1PF12.4,
 . ')',/,25X,'CALCULATION IS STOPED.')

MARY = 0

IF (ITER .NE. 1) MARY = 2

DO 120 I=1,MTOT

CALL VOLELM(MARY,I)

IF (VOL(I) .GT. 1.0E-12) GO TO 100

WRITE(6,1) I,VOL(I)

STOP

CALCULATE THE COEFFICIENTS OF X, Y, & Z IN SHAPE FUNCTIONS AND THE PARTIAL DERIVATIVES OF THE SHAPE FUNCTIONS.

100 DO 110 I=1,4

DO 110 J=1,3

110 PRTIAL(J,I) = COFACT(I,J+1,B)

CALCULATE THE ELEMENT STIFFNESS MATRIX 'ELEM' AND BUILD UP THE GLOBAL STIFFNESS MATRIX A(K,I).

F = ROELEM(I)/(VOL(I)*3b)

DO 120 I=1,4

DO 120 J=1,4

ELEM = (PRTIAL(1,I)*PRTIAL(1,J)+
 . PRTIAL(2,I)*PRTIAL(2,J)+
 . PRTIAL(3,I)*PRTIAL(3,J))*F

```
      K = NODE(I,II)
      L = NODE(J,II) - NODE(I,II) + BANDWD
120  A(K,L) = A(K,L) + ELEM
      IF (ITER .GT. 1) GO TO 170
C
C      BUILD UP THE LOAD VECTOR LOAD(I).
C
      AREAIN = 0.0
      AREAXT = 0.0
C
      DO 130 I=1,MS1
      ART(I) = AR(I)
130  AREAIN = AREAIN + ART(I)
C
      MS = MS3 + 1
      DO 140 I=MS,MSTOT
      ART(I) = AR(I)
140  AREAXT = AREAXT + ART(I)
C
      MSFLUX = MSRATE/(AREAIN*STAGRO)
      DO 150 I=1,MS1
      P = - MSFLUX*ART(I)/3
      LOAD(LBC(I)) = LOAD(LBC(I)) + P
      LOAD(MBC(I)) = LOAD(MBC(I)) + P
150  LOAD(NBC(I)) = LOAD(NBC(I)) + P
C
      MSFLUX = MSRATE/(AREAXT*STAGRO)
      DO 160 I=MS,MSTOT
      P = MSFLUX*ART(I)/3
      LOAD(LBC(I)) = LOAD(LBC(I)) + P
      LOAD(MBC(I)) = LOAD(MBC(I)) + P
160  LOAD(NBC(I)) = LOAD(NBC(I)) + P
C
      DO 180 I=1,NTOT
180  POTEN(I) = LOAD(I)
C
      RETURN
      END
```

SUBROUTINE SPLIT

THIS SUBROUTINE MODIFIES THE STIFNESS MATRIX BY INCLUDING THE
SPLITTING BOUNDARY CONTRIBUTION.

INTEGER BANDWD

REAL MSRATE,MSFLUX,LOAD,MACH2

COMMON/ASEMBL/B(4,4),VOL(3720),NODE(4,3720),A(960,406),NTL(155),

• PRTIAL(3,4),ART(155),LBC(155),MBC(155),NBC(155),
• X(960),Y(960),Z(960),LOAD(960),BANDWD,E(155),MV(155)
•, NSB(4,155),MS1,MS2,MS3,MSTOT,NTOT,JUMP1,JUMP2,NANZ,
• NRNZ,POTEN(960)
• COMMON/INOUT/INDATA,MTOT,MSRATE,EPS ILN,ITER,ITERMX,NC,STAGRD,
• J1(60),NU(60),THETA(60),ROELEM(3720),NN

IF (ITER .EQ. 1) CALL NUMBER

START THE MAIN LOOP OVER THE VOLUME (OR SURFACE) ELEMENT.

MDIF = MS1 - MS2

MS = MS1 + 1

MSS = MS2

KLM = MS

10 DO 60 II=MS,MSS

BUILD UP THE MATRIX B(I,J).

CALL VOLELM(1,II)

CALCULATE THE PARTIAL DERIVATIVES OF SHAPE FUNCTIONS

DO 20 I=1,4

DO 20 J=1,3

20 PRTIAL(J,I) = COFACT(I,J+1,B)

CALCULATE THE AREA OF THE SURFACE ELEMENT II.

AREA = SQRT(PRTIAL(1,4)**2 + PRTIAL(2,4)**2 + PRTIAL(3,4)**2)/2

IF (II.NE.KLM .OR. ITER.NE.1) GO TO 30

EVALUATE THE COEFFICIENTS OF THE PLANE EQUATION $A*X + B*Y +$
 $C*Z + D = 0$ AND THE DIRECTIONAL COSINES OF THE COMPONENTS OF
THE NORMAL VECTOR.

AX = PRTIAL(1,4)

```

BY = PRTIAL(2,4)
CZ = PRTIAL(3,4)
D = B(1,2)*(B(3,3)*B(2,4) - B(2,3)*B(3,4)) +
  B(1,3)*(B(3,4)*B(2,2) - B(2,4)*B(3,2)) +
  B(1,4)*(B(3,2)*B(2,3) - B(2,2)*B(3,3))

```

```

C
DELTA = AREA*2
IF (D.NE.0.0 .AND. D*DELTA.GT.0.0) DELTA = -DELTA
IF (D.EQ.0.0 .AND. CZ.NE.0.0 .AND. CZ*DELTA.LT.0.0) DELTA = -DELTA
IF (D.EQ.0.0 .AND. CZ.EQ.0.0 .AND. BY*DELTA.LT.0.0) DELTA = -DELTA
COSINA = AX/DELTA
COSINB = BY/DELTA
COSINC = CZ/DELTA

```

```

C
C
C
EVALUATE THE COEFFICIENTS E(I) OF THE NODAL POTENTIALS IN A
BOUNDARY ELEMENT II.

```

```

30 F = ROELEM(MV(II))/(VOL(MV(II))*18)
DO 40 I=1,4
E(I) = AREA*(COSINA*PRTIAL(1,I) + COSINB*PRTIAL(2,I) +
  COSINC*PRTIAL(3,I))*F
40 IF (MSS .EQ. MS3) E(I) = -E(I)

```

```

C
C
C
INSERT THE SURFACE INTEGRAL IN STIFFNESS MATRIX.

```

```

IJ = II - MDIF
DO 50 J=1,4
DO 50 I=1,3
K = NSB(I,II)
L = NSB(J,II) - NSB(I,IJ) + BANDWD
50 A(K,L) = A(K,L) + E(J)
60 CONTINUE

```

```

C
MDIF = -MDIF
MS = MS2 + 1
MSS = MS3
IF (MDIF .GT. 0) GO TO 10

```

```

C
C
C
INCLUDE TANGENTIAL VELOCITY IN STIFFNESS MATRIX TO INSURE
CONTINUITY THROUGH SPLITTING BOUNDARIES.

```

```

JUMP = JUMP1
K1 = NTL(1)
K2 = K1 - JUMP
MSD = (MS3 - MS2)*3
MONA = K1 + 1 - (NRNZ-1)*NANZ

```

```

C
DO 80 I=2,MSD

```



```
IF (NTL(I) .EQ. NTL(I-1)) GO TO 80
IF ( NTL(I) .GE. MONA) GO TO 70
RETURN
65 K2 = K1 - JUMP2
   JUMP = JUMP2
70 K3 = NTL(I)
   K4 = K3 - JUMP
   KT = BANDWD - K3
   L = K1 + KT
   A(K3,L) = A(K3,L) + 1.0E+15
   L = K2 + KT
   A(K3,L) = A(K3,L) - 1.0E+15
   L = K4 + KT
   A(K3,L) = A(K3,L) + 1.0E+15
   A(K3,BANDWD) = A(K3,BANDWD) - 1.0E+15
80 CONTINUE
C
666 FORMAT (10X,'A(',I3,',',I3,')=',E14.5,10X,'E(',I3,')=',E14.5)
777 FORMAT (10E12.4)
RETURN
END
```

SUBROUTINE NUMBER

C
C
C
C
C

THIS SUBROUTINE RENUMBERS THE NODES AND THE ELEMENTS ON
SPLITTING BOUNDARIES SO THAT NODES 1, 2 AND 3 ARE ON SPLITTING
SURFACES, AND REARRANGES THE NODES ON ONE SPLITTING SURFACE

INTEGER BANDWD

REAL MSRATE,MSFLUX,LOAD,MACH2

COMMON/ASEMBL/B(4,4),VOL(3720),NODE(4,3720),A(960,406),NTL(155),

• PRTIAL(3,4),ART(155),LBC(155),MBC(155),NBC(155),
• X(960),Y(960),Z(960),LOAD(960),BANDWD,E(155),MV(155)
•• NSB(4,155),MS1,MS2,MS3,MSTOT,NTOT,JUMP1,JUMP2,NANZ,
• NRNZ,POTEN(960)

C
C

DO 10 I=1,MS3
DO 10 J=1,4
10 NSB(J,I) = 0

C

MS = MS1 + 1
DO 20 J=MS,MS2
DO 20 I=1,4
IF (LBC(J) .EQ. NODE(I,MV(J))) NSB(1,J) = NODE(I,MV(J))
IF (MBC(J) .EQ. NODE(I,MV(J))) NSB(2,J) = NODE(I,MV(J))
IF (NBC(J) .EQ. NODE(I,MV(J))) NSB(3,J) = NODE(I,MV(J))
20 IF (NODE(I,MV(J)) .NE. NSB(1,J) .AND.
• NODE(I,MV(J)) .NE. NSB(2,J) .AND.
• NODE(I,MV(J)) .NE. NSB(3,J)) NSB(4,J) = NODE(I,MV(J))

C

K = 0
MS = MS2 + 1
DO 40 J=MS,MS3
DO 30 I=1,4
IF (LBC(J) .EQ. NODE(I,MV(J))) NSB(1,J) = NODE(I,MV(J))
IF (MBC(J) .EQ. NODE(I,MV(J))) NSB(2,J) = NODE(I,MV(J))
IF (NBC(J) .EQ. NODE(I,MV(J))) NSB(3,J) = NODE(I,MV(J))
30 IF (NODE(I,MV(J)) .NE. NSB(1,J) .AND.
• NODE(I,MV(J)) .NE. NSB(2,J) .AND.
• NODE(I,MV(J)) .NE. NSB(3,J)) NSB(4,J) = NODE(I,MV(J))

C

REARRANGE THE NODES IN A DECREASING VALUES ARRAY

C

DO 40 I=1,3
K = K + 1
40 NTL(K) = NSB(I,J)

C

MSD = (MS3 - MS2) * 3
MSD1 = MSD - 1

```
      K = 1
C
      DO 70 L=1,MSD1
      MNP = NTL(L)
      DO 60 M=L,MSD
      IF (NTL(M) - NTL(L)) 60,60,50
50    K = M
      NTL(L) = NTL(M)
60    CONTINUE
      NTL(K) = MNP
      K = L + 1
70    CONTINUE
C
      RETURN
      END
```

```

SUBROUTINE GAUSS
C
C SOLUTION OF LINEAR SYSTEMS OF EQUATIONS BY THE GAUSS ELIMINATION
C METHOD, FOR NON SYMETRIC BANDED SYSTEMS.
C
C A : CONTAINS THE SYSTEM MATRIX, STORED ACCORDING TO THE NON
C SYMMETRIC BANDED MATRIX
C
C POTEN : CONTAINS THE UNKNOWN POTENTIALS AFTER SOLUTION.
C
C
C INTEGER BANDWD
C REAL MSRATE,MSFLUX,LOAD,MACH2
C COMMON/ASEMBL/B(4,4),VOL(3720),NODE(4,3720),A(960,406),NTL(155),
C . PRTIAL(3,4),ART(155),LBC(155),MBC(155),NBC(155),
C . X(960),Y(960),Z(960),LOAD(960),BANDWD,E(155),MV(155)
C ., NSB(4,155),MS1,MS2,MS3,MSTOT,NTOT,JUMP1,JUMP2,NANZ,
C . NRNZ,POTEN(960)
C
C
C 1 FORMAT (1H1, 5(/), 10(1H=), * >>>> WARNING :*, /,
C . 15X, 'SINGULARITY IN ROW', I5, /,
C . 15X, 'CALCULATION IS STOPED.')
C
C
C NM1 = NTOT - 1
C DO 60 K=1,NM1
C KP1 = K + 1
C IF(ABS(A(K,BANDWD)) .LT. .00001) GO TO 80
C
C DIVIDE ROW BY DIAGONAL COEFFICIENT
C
C NI = KP1 + BANDWD - 2
C L = MIN0(NI,NTOT)
C DO 30 J=KP1,L
C K2 = BANDWD + J - K
30 A(K,K2) = A(K,K2)/A(K,BANDWD)
C POTEN(K) = POTEN(K)/A(K,BANDWD)
C
C ELIMINATE UNKNOWN FIA(K) FROM ROW I
C
C DO 50 I=KP1,L
C K1 = BANDWD + K - I
C DO 40 J=KP1,L
C K2 = BANDWD + J - I
C K3 = BANDWD + J - K
40 A(I,K2) = A(I,K2) - A(I,K1)*A(K,K3)
50 POTEN(I) = POTEN(I) - A(I,K1)*POTEN(K)

```

```
60 CONTINUE
C
C   COMPUTE LAST UNKNOWN.
C
C   IF(ABS(A(NTOT,BANDWD)) .LT. 0.0000001) GO TO 80
C   POTEN(NTOT) = POTEN(NTOT)/A(NTOT,BANDWD)
C
C   APPLY BACKSUBSTITUTION PROCESS TO COMPUTE REMAINING UNKNOWNNS.
C
C   DO 70 I=1,NM1
C   K = NTOT - I
C   KP1 = K + 1
C   NI = KP1 + BANDWD - 2
C   L = MIN0(NI,NTOT)
C   DO 70 J=KP1,L
C   K2 = BANDWD + J - K
C   70 POTEN(K) = POTEN(K) - A(K,K2)*POTEN(J)
C
C   GO TO 90
C   80 WRITE(6,1) K
C   STOP
C
C   90 RETURN
C   END
```



```

      DO 40 I=1,4
      A(NODE(I,II),1) = A(NODE(I,II),1) + 1.0
      DO 40 J=2,4
40    A(NODE(I,II),J) = A(NODE(I,II),J) + VELO(J-1)
50    CONTINUE
C
      IF (ERROR.GT.EPSILN .AND. ITER.LT.ITERMX) RETURN
C
      CALCULATE THE VELOCITY A(I,5), THE VELOCITY COMPONENTS A(I,J)
      (J=2,3,4 FOR X,Y,Z), MACH NUMBER A(I,6), NORMALIZED PRESSURE
      A(I,7), NORMALIZED DENSITY A(I,8)
C
      DO 90 I=1,NTOT
      DO 60 J=2,4
60    A(I,J) = A(I,J)/A(I,1)
C
      VSQRED = A(I,2)**2 + A(I,3)**2 + A(I,4)**2
      A(I,5) = SQRT(VSQRED)
      MACH2 = VSQRED/(SONIC - VSQRED/(2*EXPO))
      A(I,6) = SQRT(MACH2)
      A(I,8) = (1.0 + MACH2/(2*EXPO))**(-EXPO)
      A(I,7) = A(I,8)**GAMA
90    CONTINUE
C
      CRITICAL VELOCITY
      VECRIT=SQRT(2*STAGT/(EXPO*(GAMA+1.0)))
      PI=3.1416
C
      CALCULATE THE RADIAL AND THE TANGENTIAL VELOCITIES
      TANGENTIAL VELOCITY IS STORED IN A(I,2) AND THE RADIAL
      VELOCITY STORRD IN A(I,3)
C
      DO 100 K=1,NC
      JK=J1(K)
      JK1=J1(K)+NU(K)-1
      DO 100 I=JK,JK1
      VELOXY=SQRT(A(I,2)**2+A(I,3)**2)
      PHI=ATAN(A(I,3)/A(I,2))
      PSI=THETA(K)-PHI
      IF (A(I,2)*A(I,3).LT.0.0) PSI=PI-PSI
      A(I,3)=- (A(I,3)/ABS(A(I,3))) *VELOXY*COS(PSI)
100  A(I,2)=- (A(I,2)/ABS(A(I,2))) *VFLOXY*SIN(PSI)
C
      RETURN
      END

```

```
      FUNCTION COFACT(I,J,B)
C
C      FUNCTION COFACT CALCULATES THE COFACTORS OF THE MATRIX B(I,J)
C      WHERE B(I,1)=1 AND J IS ANY REAL NUMBER
C
C      DIMENSION B(4,4), C(4,4)
C
C      DO 1 M=1,4
C      DO 1 K=1,4
C      1 C(K,M) = B(K,M)
C      IF (I .EQ. 4) GO TO 3
C
C      REDUCE 4*4 MATRIX TO 3*4 MATRIX
C
C      DO 2 M=1,4
C      DO 2 K=1,3
C      2 C(K,M) = C((K+1),M)
C      3 IF (J .EQ. 4) GO TO 5
C
C      REDUCE 3*4 MATRIX TO 3*3 MATRIX
C
C      DO 4 M=J,3
C      DO 4 K=1,3
C      4 C(K,M) = C(K,(M+1))
C
C      EVALUATE THE COFACTOR
C
C      5 DETERM = C(1,3)*(C(3,2) - C(2,2)) +
C      .         C(2,3)*(C(1,2) - C(3,2)) +
C      .         C(3,3)*(C(2,2) - C(1,2))
C      L = (-1)**(I+J)
C      COFACT = DETERM * L
C
C      RETURN
C      END
```



```

SUBROUTINE VOLELM(N,K)

```

```

C
C
C
C
C
C

```

```

THIS SUBROUTINE BUILDS UP THE MATRIX B(I,J) WHERE B(I,1) = 1.0
N = 0, CALCULATES THE VOLUME VOL(K) OF AN FLEMENT K.
N = 1, BUIL UP MATRIX B FOR AN ELEMENT WITH SPLITING BOUNDARY
N = 2, BUILD UP MATRIX B FOR A VOLUME ELEMENT

```

```

INTEGER BANDWD

```

```

REAL MSRATE,MSFLUX,LOAD,MACH2

```

```

COMMON/ASEMBL/B(4,4),VOL(3720),NODE(4,3720),A(960,406),NTL(155),

```

```

. PRTIAL(3,4),ART(155),LBC(155),MBC(155),NBC(155),

```

```

. X(960),Y(960),Z(960),LOAD(960),BANDWD,E(155),MV(155)

```

```

. NSB(4,155),MS1,MS2,MS3,MSTOT,NTOT,JUMP1,JUMP2,NANZ,

```

```

. NRNZ,POTEN(960)

```

```

C
C

```

```

IF (N .NE. 1) GO TO 2

```

```

DO 1 I=1,4

```

```

B(I,1) = 1.0

```

```

B(I,2) = X(NSB(I,K))

```

```

B(I,3) = Y(NSB(I,K))

```

```

1 B(I,4) = Z(NSB(I,K))

```

```

RETURN

```

```

C

```

```

2 DO 3 I=1,4

```

```

B(I,1) = 1.0

```

```

B(I,2) = X(NODE(I,K))

```

```

B(I,3) = Y(NODE(I,K))

```

```

3 B(I,4) = Z(NODE(I,K))

```

```

IF (N .EQ. 2) RETURN

```

```

C

```

```

VOL(K) = 0.0

```

```

DO 4 I=1,4

```

```

VOLL = COFACT(I,2,B)*B(I,2)

```

```

4 VOL(K) = VOL(K) + VOLL

```

```

VOL(K) = ABS(VOL(K))/6

```

```

C

```

```

RETURN

```

```

END

```

```

C
C
C
C
      FUNCTION AR(I)
      THIS FUNCTION CALCULATES THE AREA OF A TRIANGLE IN CARTESIAN
      COORDINATES. I=NUMBER OF SURFACE ELEMENT UNDER CONSIDERATION.

      INTEGER BANDWD
      REAL MSRATE,MSFLUX,LOAD,MACH2
      COMMON/ASEMBL/B(4,4),VOL(3720),NODE(4,3720),A(960,406),NTL(155),
      .          PARTIAL(3,4),ART(155),LBC(155),MBC(155),NBC(155),
      .          X(960),Y(960),Z(960),LOAD(960),BANDWD,E(155),MV(155)
      .,
      .          NSB(4,155),MS1,MS2,MS3,MSTOT,NTOT,JUMP1,JUMP2,NANZ,
      .          NRNZ,POTEN(960)

      A1 = Y(LBC(I))*(Z(MBC(I)) - Z(NBC(I))) +
      .   Y(MBC(I))*(Z(NBC(I)) - Z(LBC(I))) +
      .   Y(NBC(I))*(Z(LBC(I)) - Z(MBC(I)))
      A2 = X(LBC(I))*(Z(MBC(I)) - Z(NBC(I))) +
      .   X(MBC(I))*(Z(NBC(I)) - Z(LBC(I))) +
      .   X(NBC(I))*(Z(LBC(I)) - Z(MBC(I)))
      A3 = X(LBC(I))*(Y(MBC(I)) - Y(NBC(I))) +
      .   X(MBC(I))*(Y(NBC(I)) - Y(LBC(I))) +
      .   X(NBC(I))*(Y(LBC(I)) - Y(MBC(I)))
      AR = SQRT(A1**2 + A2**2 + A3**2)/2

      RETURN
      END
C

```

SUBROUTINE INPUT

C
C
C

THIS SUBROUTINE READS AND WRITES THE INPUT DATA.

INTEGER BANDWD

REAL MSRATE,MSFLUX,LOAD,MACH2

COMMON/ASEMBL/B(4,4),VOL(3720),NODE(4,3720),A(960,406),NTL(155),

. PRTIAL(3,4),ART(155),LRC(155),MBC(155),NBC(155),

. X(960),Y(960),Z(960),LOAD(960),BANDWD,E(155),MV(155)

. NSB(4,155),MS1,MS2,MS3,MSTOT,NTOT,JUMP1,JUMP2,NANZ,

. NRNZ,POTEN(960)

COMMON/INOUT/INDATA,MTOT,MSRATE,EPSILN,ITER,ITERMX,NC,STAGRO,

. J1(60),NU(60),THETA(60),ROELEM(3720),NN

COMMON/PHYSI/GAMA,R,STAGT,ERROR,VELO(3)

C

1 FORMAT (6F10.0,2I5)

2 FORMAT (14I5)

3 FORMAT (1PSE14.5)

8 FORMAT (1H1,////,50X,' I N P U T D A T A ',//,

. 50X,' ',////)

9 FORMAT (33X,'TOTAL NUMBER OF ELEMENTS (MTOT) :',I6,//,

. 33X,'TOTAL NUMBER OF NODES (NTOT) :',I6,////,

. 33X,' (MS1 :',I5,//,

. 33X,' (MS2 :',I5,//,

. 33X,' SURFACE ELEMENTS AT BOUNDARIES < MS3 :',I5,//,

. 33X,' (MSTOT :',I5,//,

. 33X,' (NODIN :',I5,//,

. 33X,' (JUMP2 :',I5,////,

. 33X,' BANDWIDTH OF STIFNESS MATRIX (BANDWD) :',I5,//,

. 33X,' MAXIMUM NUMBER OF ITERATIONS (ITERMX) :',I5,//,

. 33X,' TOTAL NUMBER OF SECTIONS (NC) :',I5,//,

. 33X,' SPECIFIC HEAT RATIO (GAMA) :',F11.5,//,

. 33X,' CONVERGENCE CRITERION (EPSILN) :',F12.6,//,

. 33X,' STAGNATION TEMPERATURE (STAGT) :',F11.5,' R',//,

. 33X,' STAGNATION PRESSURE (STAGP) :',F11.5,' PSF',//,

. 33X,' IDEAL GAS CNSTANT (R) :',F11.5,' FT2/S2,R'

. ,//,33X,' MASS PATE THROUGH SYSTEM (MSRATE) :',F11.5,' SLG/S'

C
C
C

READ(5,1) MSKATE,R,GAMA,STAGT,STAGP,EPSILN,INDATA,ITERMX

READ(5,2) MTOT,NTOT,MS1,MS2,MS3,MSTOT,NANZ,NRNZ,NC,BANDWD

READ(5,2) (LBC(I),MBC(I),NBC(I),I=1,MSTOT)

READ(5,2) (NODE(1,J),NODE(2,J),NODE(3,J),NODE(4,J),J=1,MTOT)

M = MS1 + 1

READ(5,2) (MV(I),I=M,MS3)

READ(5,2) (J1(I),I=1,NC)

READ(5,2) (NU(I),I=1,NC)

```
READ(5,3) (THETA(I),I=1,NC)
READ(5,3) (X(I),I=1,NTOT)
READ(5,3) (Y(I),I=1,NTOT)
READ(5,3) (Z(I),I=1,NTOT)
```

```
C
C
C
C
```

```
INITIALIZE NORMALIZED ELEMENT DENSITIES TO BE UNITY AND CALCULATE
THE STAGNATION DENSITY.
```

```
DO 50 I=1,MTOT
50 ROFLEM(I) = 1.0
STAGRO = STAGP/(R*STAGT)
```

```
C
```

```
JUMP1 = NANZ*NRNZ
JUMP2 = LBC(MS2+1) - LBC(MS1+1)
IF (BANDWD .LT. JUMP2) BANDWD = JUMP2
IF (INDATA .EQ. 0) RETURN
```

```
C
C
C
C
C
```

```
WRITE INPUT DATA IF FLAG INDATA=1
```

```
WRITE(6,8)
WRITE(6,9) MTOT,NTOT,MS1,MS2,MS3,MSTOT,NU(1),JUMP2,BANDWD,ITERMX,
NC,GAMA,EPSILN,STAGT,STAGP,R,MSRATE
```

```
C
```

```
129 RETURN
END
```

SUBROUTINE OUTPUT

C THIS SUBROUTINE PRINTS OUT THE CALCULATED PHYSICAL PROPERTIES
 C AT THE END OF EACH ITERATION.
 C

INTEGER BANDWD

REAL MSRATE,MSFLUX,LOAD,MACH2

COMMON/ASEMBL/B(4,4),VOL(3720),NODE(4,3720),A(960,406),NTL(155),

. PRTIAL(3,4),ART(155),LBC(155),MBC(155),NBC(155),
 . X(960),Y(960),Z(960),LOAD(960),BANDWD,E(155),MV(155)
 ., NSB(4,155),MS1,MS2,MS3,MSTOT,NTOT,JUMP1,JUMP2,NANZ,
 . NRNZ,POTEN(960)

COMMON/INOUT/INDATA,MTOT,MSRATE,EPSILN,ITER,ITERMX,NC,STAGRO,
 . J1(60),NU(60),THETA(60),ROELEM(3720),NN

COMMON/PHYSI/GAMA,R,STAGT,ERRDR,VELO(3)

C
 C
 C

1 FORMAT (14I5)
 2 FORMAT (1H1,/,7X,'# NODES POTENTIALS VELOCITY-T VEL',,
 .OCITY-P VELOCITY-Z VELOCITY MACH NUM. NORM. PRES.',,
 . ' NOPM. DENS.',/)
 3 FORMAT (I9,I7,1P8E14.5)
 4 FORMAT (1P5E14.5)
 5 FORMAT (2X,'END OF SECTION',I3)
 6 FORMAT (8(/),48X,'E N D O F P R O G R A M',/,48X,27(1H_),
 . ///,33X,'CALCULATIONS ENDED :',
 . //,33X,'NUMBERS OF ITERATIONS PERFORMED : ITER =',I3,
 . //,33X,'CONVERGENCE REACHED : ERROR =',1PE8.1)

C
 C

WRITE(6,6) ITER, ERROR

J = 0

L = 53

DO 9 K=1,NC

JK = J1(K)

NK = J1(K) + NU(K) - 1

C

DO 8 I=JK,NK

J = J + 1

L = L + 1

IF (L - 53) 8,8.7

7 L = 1

WRITE(6,2)

3 WRITE(6,3) J, I, POTEN(I), (A(I,M), M=2,8)

WRITE(6,5) K

9 CONTINUE

C

AN IV G1 RELEASE 2.0

OUTPUT

DATE = 82239

04/25/19

```
C WRITE(7,1) (J1(I), I=1,NC)
C WRITE(7,1) (NU(I), I=1,NC)
C WRITE(7,4) (X(I), I=1,NTOT)
C WRITE(7,4) (Y(I), I=1,NTOT)
C WRITE(7,4) (Z(I), I=1,NTOT)
  WRITE(7,4) (POTEN(I), I=1,NTOT)
  WRITE(7,4) (A(1,6), I=1,NTOT)
  WRITE(7,4) (A(1,7), I=1,NTOT)
  WRITE(7,4) (A(1,2), I=1,NTOT)
  WRITE(7,4) (A(1,3), I=1,NTOT)
  WRITE(7,4) (A(1,4), I=1,NTOT)
C
  RETURN
  END
```

NUMERICAL EXAMPLE

A numerical example is presented to illustrate the use of the program and show the results of the computations. The flow is investigated in a radial inflow turbine for which the experimental measurements were reported in reference [8]. The mass flow rate is one lb/sec (0.454 kg/sec) and the scroll inlet section diameter is 4.88 inches (1.92 cm). The number of nodal points used in the discretization pattern was 956 placed on 24 scroll cross sections as shown in Figs. 3 and 4. The number of tetrahedral elements resulting from this discretization pattern was 2,716. The printed output from this example is given in Table 2. The first part of the output consists of the performance parameters and other input data. The second part of the output represents the results of the computations and consists of the velocity potential, the velocity components, the Mach number, the normalized density and pressure. The pressure and density are normalized with respect to their inlet stagnation values. The output data from the computed results in the various scroll cross sections. The contours of the computed velocity potentials are shown in Fig. 5. The jump in the value of the velocity potential across the splitting surfaces was found to be equal to 150 as can be seen in Fig. 5. The same figure illustrates the same slope for the potential contours on the opposite sides of the splitting surface and hence the continuation of velocity pressure and density fields. The contours of the computed velocity component in the circumferential direction are shown in Fig. 6. The measured [5] circumferential velocity components are shown in Fig. 7. In both Figs. 6 and 7, the values of the velocity component are normalized with respect to the inlet velocity.

The disagreement between the computed and measured results is mainly in the boundary layer region over the outer scroll surfaces. One can also observe some secondary flow development in the measured results. However, both boundary layer and secondary flow effects decrease with increased velocities.

The agreement between the computed and measured results near the scroll neck, in spite of the very low velocities in the case presented, with an inlet velocity of 41 m/sec, leads to the conclusion that the velocity and pressure fields in this region are not very sensitive to these effects. The flow is greatly accelerated in this region and it also acquires a radial velocity component as evidenced by the shape and density of the potential lines in the vaneless nozzle portion in Fig. 5.

REFERENCES

1. Bhinder, F.S., "Investigation of Flow in the Nozzleless Spiral Casing of a Radial Inward-Flow Gas Turbine," Proc. Instn. Mech. Engrs., Vol. 184, Part 3G(11), 1969-1970, pp. 66-71.
2. Wallace, F.J., Baines, N.C. and Whitfield, A., "A Unified Approach to the One-Dimensional Analysis and Design of Radial and Mixed Flow Turbines," ASME Paper No. 76-GT-100, 1976.
3. Hamed, A., Baskharone, E. and Tabakoff, W., "A Flow Study in Radial Inflow Turbine Scroll-Nozzle Assembly," ASME Journal of Fluids Engineering, Vol. 100, March 1978, pp. 31-36.
4. Hamed, A., Abdallah, S. and Tabakoff, W., "Radial Turbine Scroll Flow," AIAA Paper No. 77-714, presented to the AIAA 10th Fluid and Plasma Dynamics Conference, Albuquerque, NM, June 27-29, 1977.
5. Tabakoff, W., Vittal, B.V.R. and Wood, B., "Three Dimensional Flow Measurements in a Turbine Scroll," NASA CR 167920 Report, July 1982.
6. Shen, S., "Finite Element Methods in Fluid Mechanics," Annual Review of Fluid Mechanics, Vol. 9, 1977, pp. 421-445.
7. Huebner, K., The Finite Element Method for Engineers, John Wiley and Sons, 1975.
8. Tabakoff, W., Vittal, B.V.R. and Wood, B., "Three Dimensional Flow Measurements in a Turbine Scroll," NASA Report, August 1982.

TABLE 1
INPUT DATA FORMAT

Type of Input Data	Input Variables	Format
Performance, Printout and Convergence Parameters	MSRATE, R, GAMA, STAGT, STAGP, EPSILON, INDATA, ITERMX	6F10.0, 2I5
Discretization Parameters	MTOT, NTOT, MS1, MS2, MS3, MSTOT, NANZ, NRNZ, NC, BANDWD	14I5
Topology of Permanent ^{ia} Surface Elements (Inlet, Splitting, and Exit)	(LBC(I), MBC(I), NBC(I), I=1, MSTOT)	14I5
Topology of Volume Elements	(NODE(1,J), NODE(2,J), NODE(3,J), NODE(4,J), J=1, MTOT)	14I5
Volume Elements Affected by Splitting Surfaces	(MV(I), I = MS1+1, MS3)	14I5
Cross-Sectional Data	(J1(I), I = 1, NC)	14I5
	(NU(I), I = 1, NC)	14I5
	(THETA(I), I = 1, NC)	1P5E14.5
Nodal Coordinates	(X(I), I = 1, NTOT)	IP5E14.5
	(Y(I), I = 1, NTOT)	"
	(Z(I), I = 1, NTOT)	"

I N P U T D A T A

TOTAL NUMBER OF ELEMENTS (MTOT) : 3716
TOTAL NUMBER OF NODES (NTOT) : 956

SURFACE ELEMENTS AT BOUNDARIES < (MS1 : 48
(MS2 : 64
(MS3 : 80
(MSTOT : 152
(NODIN : 35
(JUMP2 : 19

BANDWIDTH OF STIFNESS MATRIX (BANDWD) : 203
MAXIMUM NUMBER OF ITERATIONS (ITERMX) : 5
TOTAL NUMBER OF SECTIONS (NC) : 24
SPECIFIC HEAT RATIO (GAMA) : 1.40000
CONVERGENCE CRITERION (EPSILN) : 0.000100
STAGNATION TEMPERATURE (STAGT) : 530.00000 R
STAGNATION PRESSURE (STAGP) : 4819.67969 PSF
IDEAL GAS CNSTANT (R) : 1716.26001 FT2/S2.R
MASS RATE THROUGH SYSTEM (MSRATE) : 0.03105SLG/S

E N D O F P R O G R A M

CALCULATIONS ENDED :
NUMBERS OF ITERATIONS PERFORMED : ITER = 2
COVERGENCE PEACHED : ERROR = 5.3E-06

TABLE 2: OUTPUT DATA, FIRST SET.

#	NOFFS	POTENTIALS	VLOCITY-T	VELOCITY-R	VELOCITY-Z	VLOCITY	MACH NUM.	NORM. PRES.	NORM. DENS.
1	1	-1.00000E+00	4.14651E+01	-2.77710E-01	-2.28283E-01	4.14566E+01	3.67506E-02	9.99056E-01	9.99326E-01
2	2	-1.00000E+00	4.14117E+01	-2.72367E-01	-2.11285E-01	4.14128E+01	3.67029E-02	9.99059E-01	9.99328E-01
3	3	-1.00000E+00	4.13564E+01	-2.59628E-01	-1.18984E-01	4.13574E+01	3.66538E-02	9.99063E-01	9.99330E-01
4	4	-1.00000E+00	4.13152E+01	-2.81513E-01	-2.90571E-02	4.13162E+01	3.66172E-02	9.99067E-01	9.99330E-01
5	5	-1.00000E+00	4.12813E+01	-3.06361E-01	7.73729E-07	4.12825E+01	3.65873E-02	9.99066E-01	9.99333E-01
6	6	-1.00000E+00	4.12505E+01	-3.90991E-01	2.27154E-01	4.12509E+01	3.65682E-02	9.99066E-01	9.99333E-01
7	7	-1.00000E+00	4.12419E+01	-5.30360E-01	4.27650E-01	4.12475E+01	3.65563E-02	9.99066E-01	9.99333E-01
8	8	-1.00000E+00	4.13272E+01	-1.75098E-01	-9.16429E-02	4.13277E+01	3.66274E-02	9.99063E-01	9.99330E-01
9	9	-1.00000E+00	4.12731E+01	-1.10277E-01	-1.01323E-01	4.12737E+01	3.65792E-02	9.99066E-01	9.99333E-01
10	10	-1.00000E+00	4.11929E+01	-9.12454E-02	-8.26440E-02	4.11931E+01	3.65081E-02	9.99069E-01	9.99335E-01
11	11	-1.00000E+00	4.11294E+01	-1.03539E-01	-5.56781E-02	4.11296E+01	3.64518E-02	9.99073E-01	9.99337E-01
12	12	-1.00000E+00	4.10882E+01	-1.34274E-01	-1.15471E-02	4.10884E+01	3.64153E-02	9.99073E-01	9.99337E-01
13	13	-1.00000E+00	4.10669E+01	-1.09113E-01	1.87591E-02	4.10673E+01	3.63966E-02	9.99076E-01	9.99340E-01
14	14	-1.00000E+00	4.11050E+01	-1.66591E-01	2.28405E-03	4.11057E+01	3.64303E-02	9.99073E-01	9.99337E-01
15	15	-1.00000E+00	4.11193E+01	-1.94307E-01	-2.57645E-02	4.11138E+01	3.64599E-02	9.99073E-01	9.99337E-01
16	16	-1.00000E+00	4.11035E+01	-1.78753E-01	-6.66670E-07	4.11037E+01	3.64289E-02	9.99073E-01	9.99337E-01
17	17	-1.00000E+00	4.10347E+01	-1.22124E-01	-6.97045E-02	4.10350E+01	3.63679E-02	9.99076E-01	9.99340E-01
18	18	-1.00000E+00	4.09653E+01	-1.19143E-01	-7.66449E-02	4.09655E+01	3.63063E-02	9.99079E-01	9.99342E-01
19	19	-1.00000E+00	4.09025E+01	-1.40298E-01	-6.06857E-02	4.09028E+01	3.62508E-02	9.99083E-01	9.99345E-01
20	20	-1.00000E+00	4.08533E+01	-1.75467E-01	-5.29004E-02	4.08537E+01	3.62072E-02	9.99086E-01	9.99347E-01
21	21	-1.00000E+00	4.08422E+01	-1.40754E-01	2.57492E-05	4.08425E+01	3.61973E-02	9.99086E-01	9.99347E-01
22	22	-1.00000E+00	4.08755E+01	-3.30522E-01	-2.64788E-03	4.08769E+01	3.62277E-02	9.99083E-01	9.99345E-01
23	23	-1.00000E+00	4.08559E+01	-2.67318E-01	-1.72209E-02	4.08564E+01	3.62099E-02	9.99086E-01	9.99347E-01
24	24	-1.00000E+00	4.07829E+01	-2.43347E-01	-3.01565E-02	4.07837E+01	3.61451E-02	9.99089E-01	9.99349E-01
25	25	-1.00000E+00	4.07303E+01	-2.22368E-01	-5.73662E-02	4.07310E+01	3.60984E-02	9.99089E-01	9.99349E-01
26	26	-1.00000E+00	4.06853E+01	-1.99889E-01	-7.72312E-02	4.06859E+01	3.60585E-02	9.99093E-01	9.99352E-01
27	27	-1.00000E+00	4.06521E+01	-1.89407E-01	-7.89407E-02	4.06527E+01	3.60290E-02	9.99093E-01	9.99352E-01
28	28	-1.00000E+00	4.06306E+01	-1.44093E-01	3.52859E-05	4.06309E+01	3.60097E-02	9.99096E-01	9.99354E-01
29	29	-1.00000E+00	4.07084E+01	1.77200E-01	-3.53218E-01	4.07103E+01	3.60801E-02	9.99089E-01	9.99349E-01
30	30	-1.00000E+00	4.06371E+01	1.29026E-04	-7.39117E-07	4.06372E+01	3.60153E-02	9.99093E-01	9.99352E-01
31	31	-1.00000E+00	4.05544E+01	-1.03290E-04	-4.56409E-02	4.05544E+01	3.59419E-02	9.99099E-01	9.99357E-01
32	32	-1.00000E+00	4.05079E+01	1.27186E-05	-1.29428E-02	4.05079E+01	3.59007E-02	9.99099E-01	9.99357E-01
33	33	-1.00000E+00	4.05003E+01	-1.03152E-04	1.37916E-02	4.05003E+01	3.58939E-02	9.99099E-01	9.99357E-01
34	34	-1.00000E+00	4.05164E+01	1.27213E-05	1.68006E-02	4.05164E+01	3.59082E-02	9.99099E-01	9.99357E-01
35	35	-1.00000E+00	4.05270E+01	1.28677E-04	7.34329E-05	4.05270E+01	3.59176E-02	9.99099E-01	9.99357E-01
END OF SECTION 1									
36	36	7.18763E+00	4.09895E+01	-3.96642E-02	-4.94801E-01	4.09925E+01	3.63303E-02	9.99079E-01	9.99342E-01
37	37	7.17864E+00	4.07953E+01	1.04591E-01	-5.02956E-01	4.07935E+01	3.61593E-02	9.99086E-01	9.99347E-01
38	38	7.17281E+00	4.05365E+01	3.17901E-02	-2.80113E-01	4.05375E+01	3.59269E-02	9.99099E-01	9.99357E-01
39	39	7.16706E+00	4.04120E+01	-1.63282E-02	-2.00487E-01	4.04125E+01	3.58161E-02	9.99103E-01	9.99359E-01
40	40	7.16065E+00	4.07905E+01	-1.10038E-01	-1.36097E-03	4.03907E+01	3.57968E-02	9.99106E-01	9.99361E-01
41	41	7.15203E+00	4.04340E+01	-3.55913E-01	1.41763E-01	4.04358E+01	3.58367E-02	9.99103E-01	9.99359E-01
42	42	7.13969E+00	4.06861E+01	-5.70675E-01	2.31441E-01	4.06908E+01	3.60628E-02	9.99093E-01	9.99352E-01
43	43	7.15937E+00	4.13281E+01	-1.07626E-01	-3.80404E-01	4.13100E+01	3.66295E-02	9.99063E-01	9.99330E-01
44	44	7.14420E+00	4.12348E+01	-8.28834E-02	-4.19080E-01	4.12370E+01	3.65470E-02	9.99066E-01	9.99331E-01
45	45	7.12620E+00	4.10419E+01	-3.48614E-02	-3.29622E-01	4.10432E+01	3.63752E-02	9.99076E-01	9.99340E-01
46	46	7.11289E+00	4.09241E+01	-8.14002E-02	-2.42535E-01	4.09249E+01	3.62703E-02	9.99083E-01	9.99345E-01
47	47	7.10596E+00	4.08363E+01	-1.70098E-01	-1.00002E-01	4.08368E+01	3.61922E-02	9.99086E-01	9.99347E-01
48	48	7.10056E+00	4.07710E+01	-3.26994E-01	-4.34806E-02	4.07724E+01	3.61351E-02	9.99089E-01	9.99349E-01
49	49	7.10890E+00	4.08758E+01	-5.04404E-01	1.91217E-01	4.08794E+01	3.62300E-02	9.99081E-01	9.99345E-01
50	50	7.12317E+00	4.17365E+01	-2.85654E-02	-4.62786E-01	4.17384E+01	3.69915E-02	9.99046E-01	9.99318E-01
51	51	7.11230E+00	4.14892E+01	-1.12042E-01	-2.67369E-01	4.14902E+01	3.67715E-02	9.99056E-01	9.99326E-01
52	52	7.09876E+00	4.13442E+01	-7.30094E-02	-3.74060E-01	4.13456E+01	3.66437E-02	9.99063E-01	9.99330E-01
53	53	7.08449E+00	4.11905E+01	-7.89445E-02	-3.18591E-01	4.11918E+01	3.65069E-02	9.99069E-01	9.99335E-01

OUTPUT DATA, SECOND SET

#	NODES	POTENTIALS	VELOCITY-T	VELOCITY-R	VELOCITY-Z	VELOCITY	MACH NUM.	NDPM. PRES.	NORM. DENS.
54	54	7.07102E+00	4.10321E+01	-1.47512E-01	-3.03914E-01	4.10335E+01	3.63666E-02	9.99076E-01	9.99340E-01
55	55	7.06279E+00	4.08643E+01	-2.67546E-01	-2.56200E-01	4.08660E+01	3.62191E-02	9.99083E-01	9.99345E-01
56	56	7.05251E+00	4.08121E+01	-3.69517E-01	-2.50362E-02	4.08137E+01	3.61718E-02	9.99086E-01	9.99347E-01
57	57	7.04337E+00	4.20381E+01	-3.87113E-01	-4.42598E-01	4.20422E+01	3.72608E-02	9.99029E-01	9.99307E-01
58	58	7.07536E+00	1.16499E+01	-4.60355E-01	-1.77582E-01	4.16519E+01	3.69148E-02	9.99049E-01	9.99321E-01
59	59	7.05986E+00	4.14941E+01	-4.56743E-01	-2.95976E-01	4.14976E+01	3.67780E-02	9.99056E-01	9.99326E-01
60	60	7.04837E+00	4.13149E+01	-4.24784E-01	-3.12191E-01	4.13183E+01	3.66191E-02	9.99063E-01	9.99330E-01
61	61	7.03397E+00	4.11347E+01	-3.65691E-01	-3.94559E-01	4.11313E+01	3.64595E-02	9.99073E-01	9.99337E-01
62	62	7.02370E+00	4.09277E+01	-3.28719E-01	-4.13059E-01	4.09312E+01	3.62759E-02	9.99083E-01	9.99345E-01
63	63	7.00910E+00	4.07786E+01	-3.42145E-01	-1.27613E-01	4.07902E+01	3.61421E-02	9.99089E-01	9.99349E-01
64	64	7.02412E+00	4.17335E+01	-6.34015E-01	-2.37633E-01	4.17830E+01	3.70364E-02	9.99043E-01	9.99316E-01
65	65	7.00712E+00	4.13802E+01	-6.08909E-01	-3.98652E-02	4.13847E+01	3.66779E-02	9.99059E-01	9.99328E-01
66	66	6.98909E+00	4.12168E+01	-5.22607E-01	-1.13506E-01	4.12203E+01	3.65322E-02	9.99069E-01	9.99335E-01
67	67	6.97795E+00	4.10579E+01	-4.74616E-01	-1.70427E-01	4.10610E+01	3.63909E-02	9.99076E-01	9.99340E-01
68	68	6.97480E+00	4.09390E+01	-4.35796E-01	-2.13094E-01	4.09419E+01	3.62854E-02	9.99079E-01	9.99347E-01
69	69	6.97819E+00	4.08258E+01	-3.86706E-01	-3.16890E-01	4.08288E+01	3.61852E-02	9.99086E-01	9.99347E-01
70	70	6.98991E+00	4.07109E+01	-3.84171E-01	-1.42712E-01	4.07130E+01	3.60825E-02	9.99089E-01	9.99346E-01
END OF SECTION 2									
71	71	1.52192E+01	3.91744E+01	3.18266E+00	-7.56709E-01	3.92610E+01	3.47953E-02	9.99156E-01	9.99397E-01
72	72	1.51031E+01	3.88190E+01	3.38950E+00	-8.37512E-01	3.89757E+01	3.45424E-02	9.99166E-01	9.99404E-01
73	73	1.49977E+01	3.83258E+01	3.24065E+00	-4.70970E-01	3.84555E+01	3.40901E-02	9.99189E-01	9.99421E-01
74	74	1.49450E+01	3.91437E+01	3.15642E+00	-5.57159E-01	3.82782E+01	3.39240E-02	9.99196E-01	9.99426E-01
75	75	1.49310E+01	3.82690E+01	2.93911E+00	-3.28313E-02	3.83813E+01	3.40171E-02	9.99193E-01	9.99423E-01
76	76	1.49637E+01	3.86215E+01	2.26045E+00	-1.38315E-01	3.86879E+01	3.42872E-02	9.99179E-01	9.99414E-01
77	77	1.50069E+01	3.90756E+01	1.68157E+00	-6.22070E-01	3.91167E+01	3.46674E-02	9.99179E-01	9.99399E-01
78	78	1.52496E+01	4.03176E+01	2.47146E+00	-7.37929E-01	4.04000E+01	3.58050E-02	9.99106E-01	9.99361E-01
79	79	1.52064E+01	4.02937E+01	1.98258E+00	-1.01768E+00	4.01548E+01	3.57650E-02	9.99106E-01	9.99361E-01
80	80	1.51024E+01	3.99132E+01	2.10123E+00	-8.19441E-01	3.99768E+01	3.54299E-02	9.99123E-01	9.99373E-01
81	81	1.50575E+01	3.97281E+01	1.98098E+00	-6.86289E-01	3.97834E+01	3.52584E-02	9.99133E-01	9.99380E-01
82	82	1.50222E+01	3.96520E+01	1.78162E+00	-4.41249E-01	3.96945E+01	3.51796E-02	9.99136E-01	9.99383E-01
83	83	1.50257E+01	3.97274E+01	1.38599E+00	-4.64410E-01	3.97543E+01	3.52326E-02	9.99133E-01	9.99380E-01
84	84	1.50103E+01	3.97716E+01	2.97724E-01	1.61471E-01	3.97730E+01	3.52492E-02	9.99133E-01	9.99380E-01
85	85	1.53616E+01	4.19397E+01	2.92792E+00	-1.00604E+00	4.20538E+01	3.72711E-02	9.99029E-01	9.99307E-01
86	86	1.52977E+01	4.17392E+01	2.01143E+00	-7.36788E-01	4.17941E+01	3.70409E-02	9.99043E-01	9.99316E-01
87	87	1.52405E+01	4.16064E+01	2.01486E+00	-9.66585E-01	4.16664E+01	3.69277E-02	9.99049E-01	9.99321E-01
88	88	1.51848E+01	4.14062E+01	1.91611E+00	-9.45031E-01	4.14613E+01	3.67459E-02	9.99056E-01	9.99326E-01
89	89	1.51398E+01	4.11694E+01	1.69564E+00	-9.97424E-01	4.12163E+01	3.65287E-02	9.99069E-01	9.99335E-01
90	90	1.50832E+01	4.09300E+01	1.33544E+00	-9.79833E-01	4.09635E+01	3.63045E-02	9.99079E-01	9.99342E-01
91	91	1.50044E+01	4.05692E+01	4.98247E-01	-5.17966E-01	4.05756E+01	3.59607E-02	9.99096E-01	9.99354E-01
92	92	1.54691E+01	4.37507E+01	2.39792E+00	-1.53908E+00	4.38434E+01	3.88577E-02	9.99046E-01	9.99247E-01
93	93	1.53960E+01	4.33231E+01	1.36915E+00	-8.38337E-01	4.33529E+01	3.84228E-02	9.99069E-01	9.99264E-01
94	94	1.53393E+01	4.33624E+01	1.09032E+00	-1.11853E+00	4.33906E+01	3.84562E-02	9.99066E-01	9.99261E-01
95	95	1.52712E+01	4.31010E+01	1.01548E+00	-1.13397E+00	4.31279E+01	3.82233E-02	9.99079E-01	9.99271E-01
96	96	1.52040E+01	4.26860E+01	1.05894E+00	-1.40832E+00	4.27224E+01	3.78638E-02	9.99092E-01	9.99285E-01
97	97	1.51110E+01	4.20846E+01	1.09141E+00	-1.49604E+00	4.21253E+01	3.73345E-02	9.99026E-01	9.99304E-01
98	98	1.50267E+01	4.13471E+01	5.64901E-01	-8.85083E-01	4.14005E+01	3.66919E-02	9.99059E-01	9.99328E-01
99	99	1.54644E+01	4.42665E+01	4.04073E-01	-1.42438E+00	4.42913E+01	3.92547E-02	9.98923E-01	9.99230E-01
100	100	1.53954E+01	4.37458E+01	1.64251E-03	-9.92710E-01	4.37571E+01	3.87811E-02	9.98949E-01	9.99249E-01
101	101	1.53045E+01	4.36368E+01	-4.36754E-01	-9.58598E-01	4.36995E+01	3.87301E-02	9.98953E-01	9.99252E-01
102	102	1.52192E+01	4.33793E+01	-5.61985E-01	-1.05208E+00	4.33958E+01	3.84609E-02	9.98966E-01	9.99261E-01
103	103	1.51650E+01	4.29370E+01	-5.18822E-01	-1.24304E+00	4.29591E+01	3.80728E-02	9.98989E-01	9.99278E-01
104	104	1.51107E+01	4.23267E+01	-2.90787E-01	-1.61529E+00	4.23585E+01	3.75412E-02	9.99016E-01	9.99297E-01
105	105	1.50588E+01	4.16046E+01	-1.71164E-01	-9.81247E-01	4.16765E+01	3.69366E-02	9.99046E-01	9.99318E-01
END OF SECTION 3									
106	106	2.66447E+01	3.59114E+01	3.01939E+00	1.54968E-01	3.60384E+01	3.19386E-02	9.99289E-01	9.99492E-01

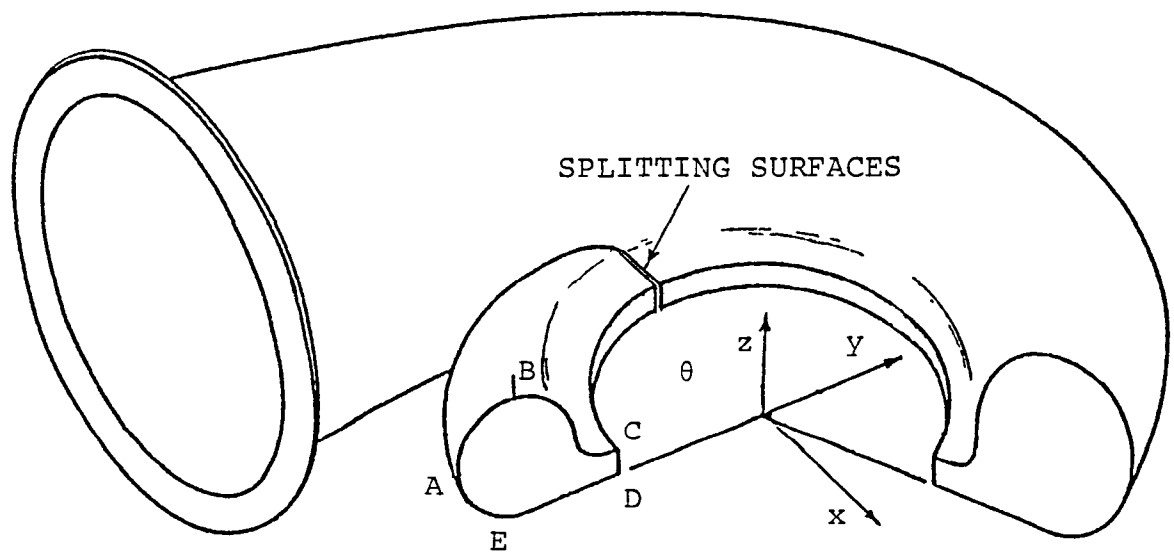


FIG. 1. SCROLL SCHEMATIC SHOWING THE COORDINATES AND THE SPLITTING SURFACES.

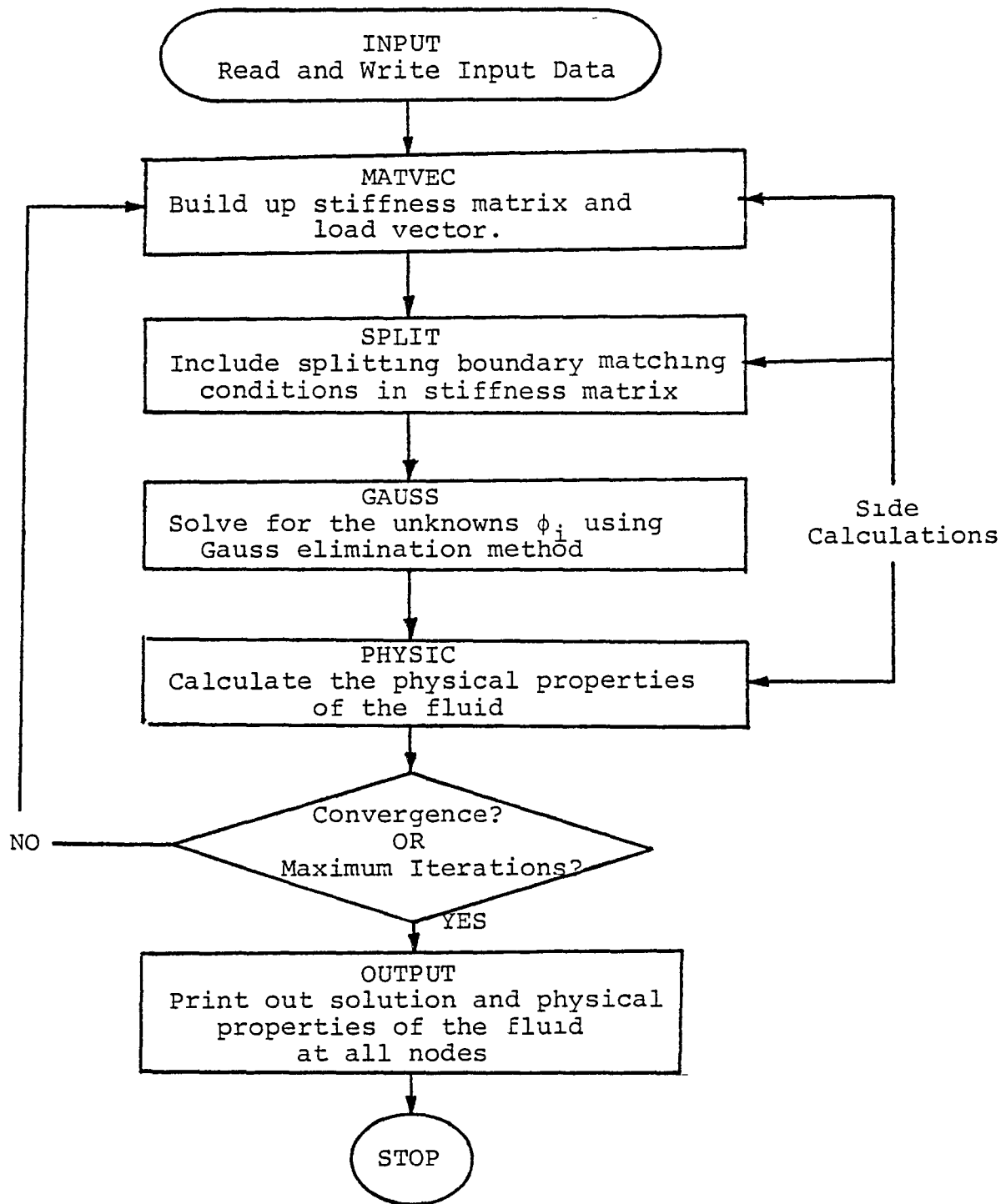


FIG. 2. STRUCTURE OF THE PROGRAM.

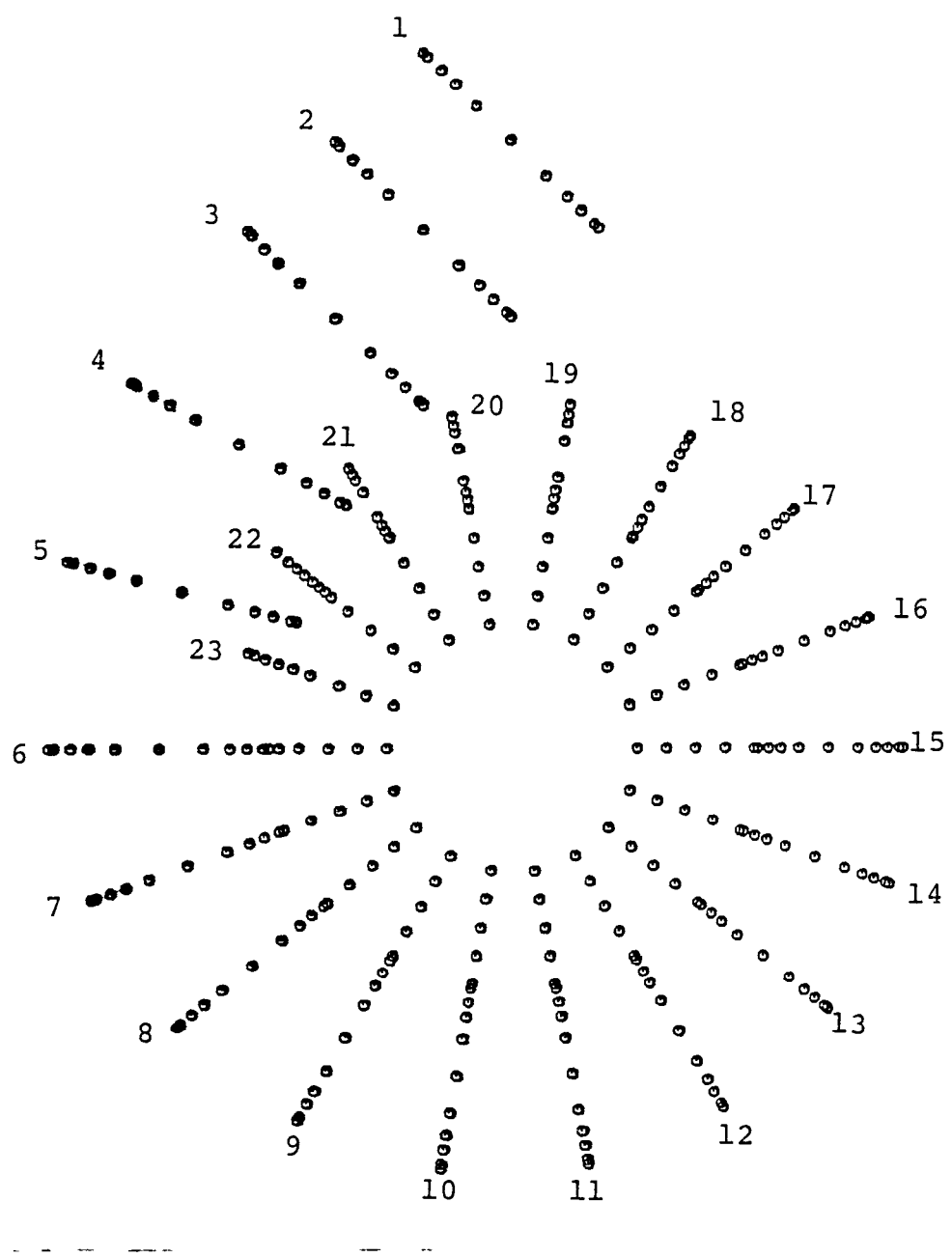


FIG. 3. NODAL PLACEMENT ON THE SCROLL SURFACE ABC.

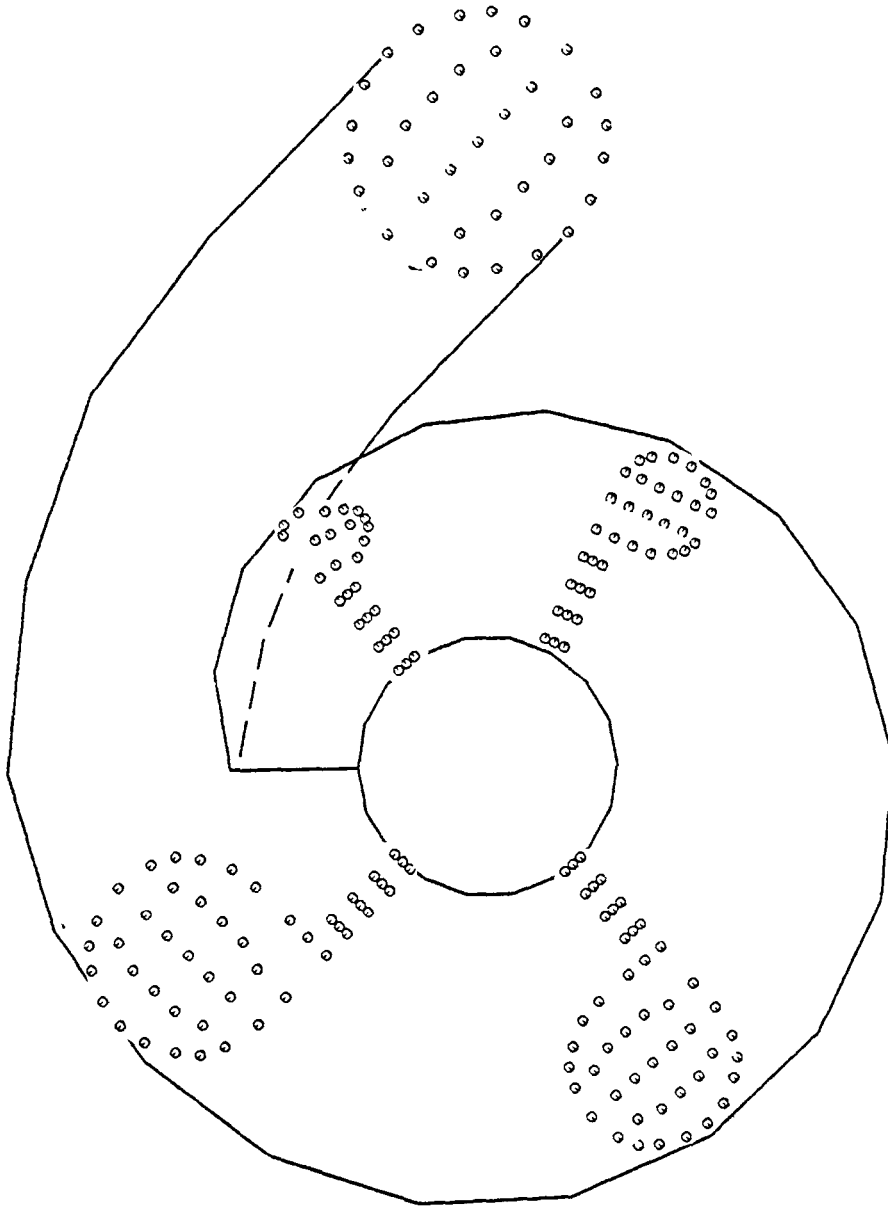


FIG. 4. NODAL PLACEMENT IN SCROLL CROSS SECTION.

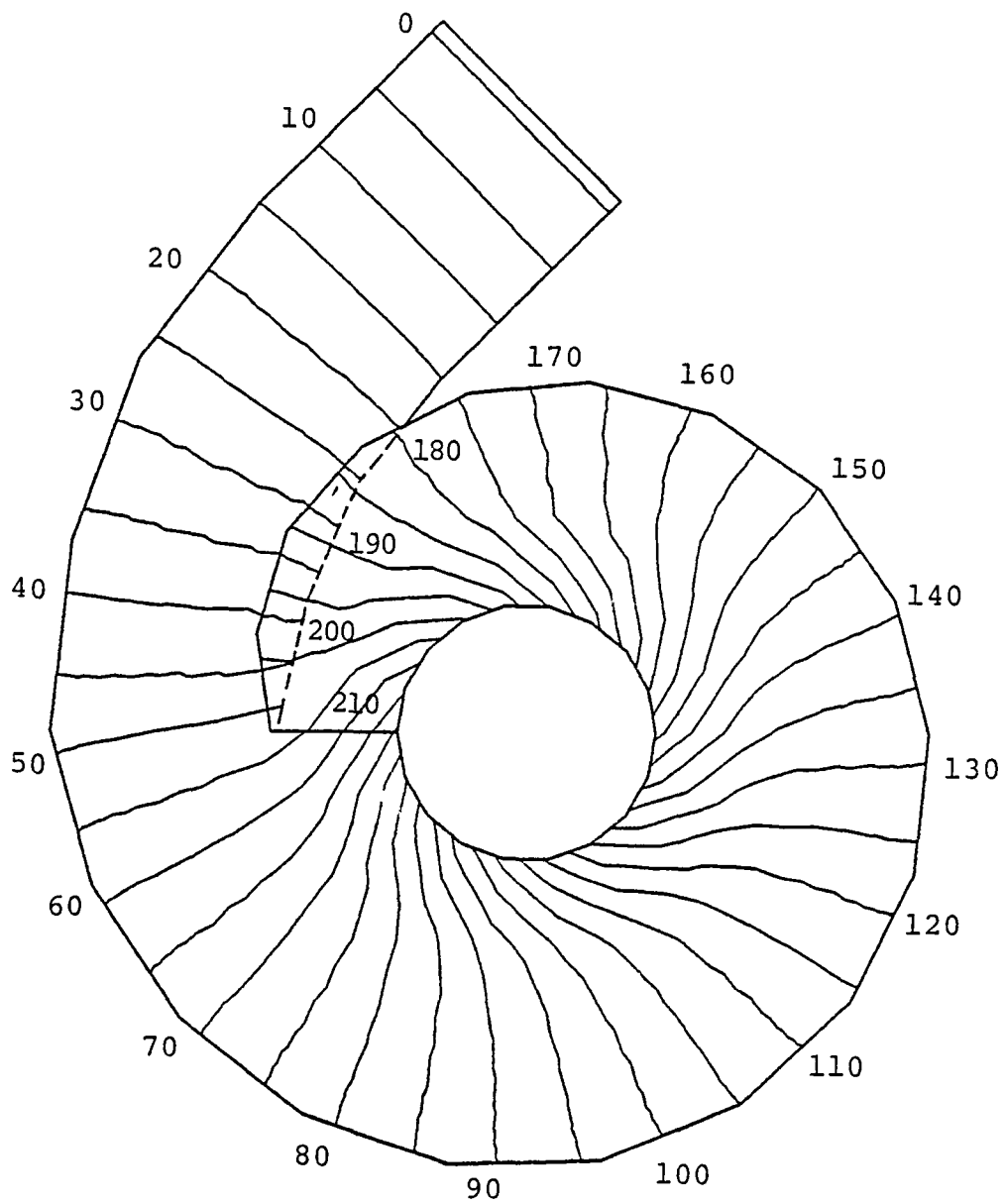
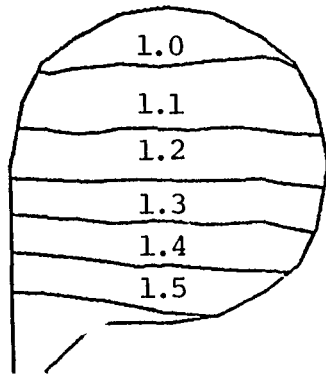
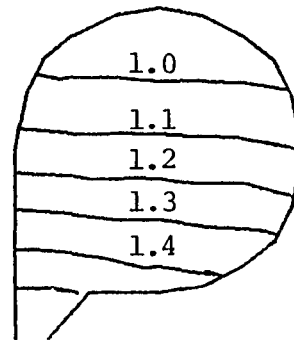


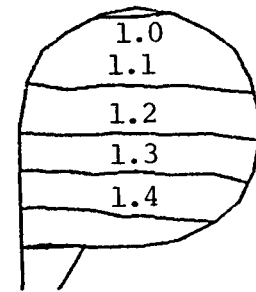
FIG. 5. VELOCITY POTENTIAL CONTOURS ON SCROLL SURFACE AED.



SECTION NO. 8
($\theta = 40^\circ$)



SECTION NO. 12
($\theta = 120^\circ$)



SECTION NO. 15
($\theta = 180^\circ$)

FIG. 6. CONTOURS OF COMPUTED CIRCUMFERENTIAL VELOCITY COMPONENT.

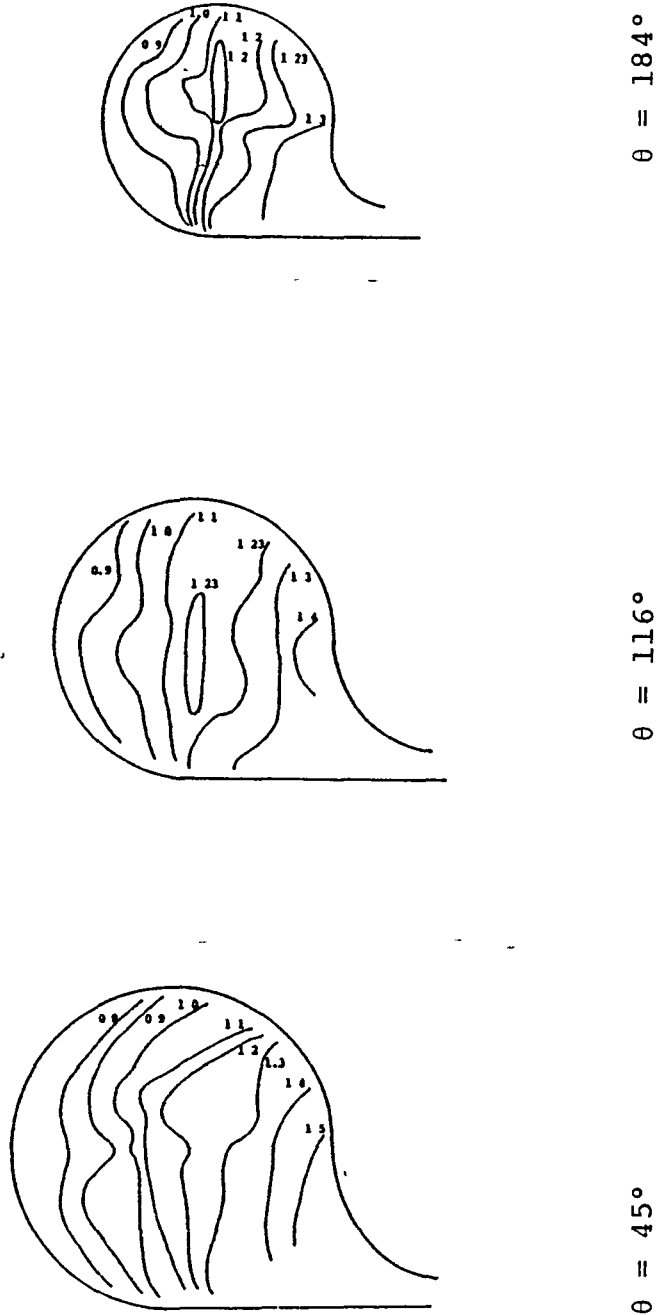


FIG. 7. MEASURED CIRCUMFERENTIAL VELOCITY COMPONENTS (REF. 5).

APPENDIX A

DERIVATION OF THE ELEMENT EQUATIONS

The simple four node linear tetrahedral element is used in the present analysis. In this case the unknown velocity potential field in an element is given by the following equation:

$$\phi^e = \sum_{i=1}^4 \phi_i N_i \quad (\text{A.1})$$

where ϕ_i are the unknown velocity potentials at the elements four nodes, and

N_i are the linear interpolation functions ($i=1,2,3,4$).

The element equation is given by equation (5) which is rewritten below:

$$\int_{V^e} \nabla N_i \cdot (\rho \nabla [N] \{\phi\}^e) dV = \int_{A^e} N_i \rho \frac{\partial \phi}{\partial n} dA \quad (\text{A.2})$$

The above equation will be written in a different form as follows:

$$[K]^e \{\phi\}^e = \{P\}^e \quad (\text{A.3})$$

The Stiffness Matrix

The coefficients K_{ij} of the element stiffness matrix can be shown [6, 7] to be given by:

$$K_{ij} = \rho \left(\frac{\partial N_i}{\partial x} \frac{\partial N_j}{\partial x} + \frac{\partial N_i}{\partial y} \frac{\partial N_j}{\partial y} + \frac{\partial N_i}{\partial z} \frac{\partial N_j}{\partial z} \right) V^e \quad (\text{A.4})$$

An element matrix $[B]^e$, is defined to contain the geometric properties of the element as follows:

$$[B]^e = \begin{vmatrix} 1 & x_1 & y_1 & z_1 \\ 1 & x_2 & y_2 & z_2 \\ 1 & x_3 & y_3 & z_3 \\ 1 & x_4 & y_4 & z_4 \end{vmatrix} \quad (A.5)$$

In the following derivations, it will be assumed that the local numbering of the volume element nodes is such that the first three are numbered counterclockwise in ascending order when viewed from the fourth node [7].

Using linear interpolation functions,

$$N_i = a_i x + b_i y + c_i z + d_i \quad (A.6)$$

it can be shown that the derivatives of the interpolation functions are given by [7],

$$\frac{\partial N_i}{\partial x} = a_i = \frac{1}{6V^e} \text{cofactor } (B_{x_i})$$

$$\frac{\partial N_i}{\partial y} = b_i = \frac{1}{6V^e} \text{cofactor } (B_{y_i})$$

$$\frac{\partial N_i}{\partial z} = c_i = \frac{1}{6V^e} \text{cofactor } (B_{z_i}) \quad (A.7)$$

The element stiffness matrix is then given by

$$K_{ij} = \rho \left(\frac{a_i a_j + b_i b_j + c_i c_j}{36V^e} \right) \quad (A.8)$$

where

$$V^e = \frac{1}{6} \det [B]^e \quad (A.9)$$

Equation (A.8) is used to build up the global matrix of coefficients in subroutine MATVEC.

The load vector surface integrals on the right hand side of equation (A.2) are only evaluated for the surfaces of the element that lie on the external boundaries with mass flow across. The contribution of the surface element to the load vector corresponding to each of its 3 nodes is given by:

$$P = f \frac{A^e}{3} \tag{A.10}$$

where f is the mass flux into the element surface whose area is equal to A^e . Equation (A.10) is used to build up the components of the load vector in subroutine MATVEC.

The Flow Velocity

The velocity in the linear tetrahedral elements can be expressed in terms of the derivative of the interpolation functions and velocity potential at element nodes as follows:

$$v_x = \sum_{i=1}^4 \frac{\partial N_i}{\partial x} \phi_i = a_i \phi_i$$

$$v_y = \sum_{i=1}^4 \frac{\partial N_i}{\partial y} \phi_i = b_i \phi_i$$

$$v_z = \sum_{i=1}^4 \frac{\partial N_i}{\partial z} \phi_i = c_i \phi_i \tag{A.11}$$

where the repeated indices imply summation over $i=1$ to 4.

APPENDIX B

THE MATCHING CONDITIONS AT THE SPLITTING SURFACES

The splitting surfaces are introduced in the solution domain in order to be able to handle the mathematically multi-valued velocity potential in the numerical solution. They can be arbitrarily placed in the flow field extending from the point where two streams of different histories join at the scroll lip, to the exit station. Nodes with different global numbers, but which have the same coordinates are placed opposite each other on the two splitting surfaces. The velocity potentials at each two nodes will generally be different, thus allowing for a velocity potential discontinuity in the numerical solution. Conditions are introduced in the equations to match the mass flow across the splitting boundaries and the difference between the velocity potential values of the opposite nodes on the splitting surfaces.

The first condition imposed in the numerical solution is the matching of the weighted mass flow across the splitting surfaces. Across an element's surface, s^e , on the splitting boundary, the weighted mass flow is given by:

$$w_s^e = \int_{A_s^e} N_i \rho \frac{\partial \phi^e}{\partial n} d A_s^e \quad (B.1)$$

where $\partial \phi^e / \partial n$ is derivative of the velocity potential normal to the surface area A_s^e . This derivative can be expressed in terms of the x , y and z derivatives of ϕ and the direction cosines α , β and γ of the normal to the surface A_s as follows:

$$\frac{\partial \phi^e}{\partial n} = \alpha \sum_1^4 \phi_1^e \frac{\partial N_1}{\partial x} + \beta \sum_1^4 \phi_i^e \frac{\partial N_i}{\partial y} + \gamma \sum_1^4 \phi_i^e \frac{\partial N_i}{\partial z} \quad (B.2)$$

Substituting equation (B.2) into (B.1) and using equation (A.7) one obtains the following expression for the contribution of the weighted mass flow across the splitting surface to each of the opposite surface nodes.

$$E = \frac{1}{3} \sum_1^4 \rho (\alpha a_1 + \beta b_1 + \gamma c_1) \phi_i A_s^e \quad (B.3)$$

The direction cosines α , β and γ of the normal to the surface of the element on the splitting boundary can be expressed in terms of the coordinates of its three nodal points. If the first three nodes of a volume element lie on the splitting surface and the fourth is an internal node, it can be shown that the direction cosines α , β and γ are proportional to cofactor B_{x_4} , cofactor B_{y_4} and cofactor b_{z_4} respectively. The proportionality constant is determined from

$$\alpha^2 + \beta^2 + \gamma^2 = 1 \quad . \quad (B.4)$$

The second condition is imposed to match the velocity potential difference between each two opposite nodes on the splitting surfaces. In the following derivations and discussions, it will be assumed that if the nodes of the volume element on one of the splitting boundaries are i, j, k , etc., the opposite nodes on the other splitting boundary are i', j', k' , etc. The mass flow matching condition is introduced by adding $\dot{m}_s/3$ to the global matrix coefficients in the columns corresponding to the nodes ($i = 1, 2, 3, 4$) in the rows ($i = 1', 2', 3', 4'$) in subroutine SPLIT. The same process is repeated reversing the roles of the primed and unprimed sides.

The second matching conditions insures the same difference between the velocity potential values of the opposite nodes on the splitting surface.

$$\phi_i - \phi_i' = \phi_j - \phi_j' \quad . \quad (B.5)$$

This condition is introduced by modifying the coefficients of the row corresponding to the node i on one side of the splitting boundaries. This is accomplished by replacing the diagonal coefficient and the coefficient in column j' by a very large number and those in columns i' and j by equal but negative large numbers.

APPENDIX C
NOMENCLATURE

A	Surface area.
B	The element matrix.
K	Matrix of coefficients or stiffness matrix.
\dot{m}	mass flow rate.
N	Interpolation function.
P	Load vector
R	Gas constant.
T	Temperature.
x,y,z	Cartesian coordinates
α, β, γ	Direction cosines of the normal to a surface
γ	Specific heat ratio.
ρ	Gas density.
ϕ	Velocity potential

Superscripts

e Refers to the volume element.

Subscripts

i,j Refers to the nodes of an element or the indices
 of the corresponding stiffness matrix.

s Refers to the splitting surfaces.

End of Document